New Materials, Compounds and Applications
Vol.8, No.3, 2024, pp.402-410
https://doi.org/10.62476/nmca83402

# THE PHASE DIAGRAM OF THE $In_2Se_3$-$SrInSe_2$ SYSTEM AND THE PHOTO- AND ELECTROPHYSICAL PROPERTIES OF THE OBTAINED PHASES

**N.I. Yagubov[1], A.N. Sultanova[1*], I.I. Aliyev[2], L.M. Gurbanova[3], C.A. Ahmedova[4], N.A. Aliyeva[5]**

[1]Baku State University, Baku, Azerbaijan
[2]Institute of Catalysis and Inorganic Chemistry named after M.F. Nagiyev, Ministry of Science and Education, Baku, Azerbaijan
[3]Western Caspian University, Baku, Azerbaijan
[4]Faculty of Science and Literature, Faculty of Chemistry, Adiyaman University, Turkiye
[5]Institute of Physics, Ministry of Science and Education, Baku, Azerbaijan

**Abstract.** Using the methods of physico-chemical analysis: differential-thermal analysis (DTA), X-ray diffraction (XRD), microstructural analysis (MSA), as well as density and microhardness measurements, the chemical interaction in the $In_2Se_3$-$SrInSe_2$ system was studied and its phase T-x diagram was constructed. The phase diagram of the system is quasi-binary and eutectic. The composition of the eutectic formed between the compounds $In_2Se_3$ and $SrInSe_2$ is 35 mol % $SrInSe_2$, with a melting point of 720°C. According to the results of the microstructural analysis in a system based on the $In_2Se_3$ compound, the solid solution region reaches up to 7 mol % $SrInSe_2$ and based on $SrInSe_2$, the solubility is 10 mol % $In_2Se_3$. The temperature dependences of electrical conductivity and thermoelectric driving force, as well as the spectral dependence of photoconductivity of solid solution alloys $(In_2Se_3)_{1-x}(SrInSe_2)_x$ (x=0.01; 0.03; 0.05), have been studied.

***Keywords:*** *Phase, quasi-binary, eutectic, solid solution, density.*

***Corresponding Author:*** *Aytan Sultanova, Baku State University, Z. Khalilov, 23, Baku, Azerbaijan, e-mail: aytansultanova26@gmail.com*

***Received:*** *4 August 2024;* ***Accepted:*** *4 October 2024;* ***Published:*** *10 December 2024.*

## 1. Introduction

The alkaline earth chalcogenide additives are potent activators; they are widely used to prepare phosphors with luminescent properties (Wauters *et al*., 2000; Wu *et al*., 2002; Tagiev *et al*., 2000; Van Haecke *et al*., 2004; 2005; Chartier *et al*., 2003). Systems based on strontium chalcogenides have been less studied than calcium chalcogenides. There are only several pieces of information in the literature about systems consisting of strontium chalcogenides (Andreev *et al*., 2008; 1991; Yagubov *et al*., 2023a; 2023b; 2022). Since elements of this group are highly reactive, they are also used as neutron moderators in nuclear reactors. Many systems involving indium chalcogenides have been studied (Mahammadrahimova *et al*., 2018; Aliyev *et al*., 2019; 2020; Mammadov, 2019). Indium chalcogenides are also semiconductor materials with photoelectric properties (Liu *et al*.,

**How to cite (APA):**
Yagubov, N.I., Sultanova, A.N., Aliyev, I.I., Gurbanova, L.M., Ahmedova, C.A. & Aliyeva, N.A. (2024). The phase diagram of the $In_2Se_3$-$SrInSe_2$ system and the photo- and electrophysical properties of the obtained phases. *New Materials, Compounds and Applications*, *8*(3), 402-410 https://doi.org/10.62476/nmca83402

2022; Island *et al*., 2015; Jacobs-Gedrim *et al*., 2014; Zhai *et al*., 2010; Xue *et al*., 2020; Zhou *et al*., 2019; Ho *et al*., 2013). From this point of view, exploring the interactions between $In_2Se_3$ and $SrInSe_2$ is of scientific and practical importance.

This work aims to study the photo- and electrophysical properties of phases obtained by analyzing the interactions in the $In_2Se_3$-$SrInSe_2$ system and constructing its phase diagram.

The $In_2Se_3$ compound melts congruently at 900°C and crystallizes in the hexagonal syngony, with lattice parameters: $a$=16.00; $c$=19.24 Å; its density was found to be 6.67 g/cm$^3$, microhardness 600 MPa (Lyakishev, 2001). In the $In_2Se_3$ compound, the following phase transitions were observed: $\alpha \leftrightarrow \beta$ (200°C), $\beta \leftrightarrow \gamma$ (650°C), $\gamma \leftrightarrow \delta$ (750°C). The $SrInSe_2$ compound melts congruently at 1180°C; its density and microhardness were found to be $\rho$=5.13 g/cm$^3$ and H$\mu$=1080 MPa, respectively (Yagubov *et al*., 2024).

## 2. Experimental part

The synthesis of alloys of the $In_2Se_3$-$SrInSe_2$ system was carried out by the method of joint melting of the $In_2Se_3$ and $SrInSe_2$ components in a quartz ampoule with air inflow to a pressure of 0.133 Pa. The synthesis of alloys was carried out in the temperature range of 1000-1100°C. The alloys were subjected to heat treatment for 150 hours at 800°C to homogenize them. Then, we studied the samples with the use of physicochemical analysis (DTA, XRD, MSA measurement of density and microhardness).

Differential thermal analysis (DTA) of the alloys was carried out using a TERMOSKAN-2 device. Chromel-alumel was used as a thermocouple; the heating rate was 5$^o$C/min.

X-ray phase analysis (XPA) was carried out on a D2 PHASER X-ray diffractometer. In this case, CuK$\alpha$ radiation and a Ni filter were used. The microstructure of the samples was analyzed using a MIM-8 microscope. A chromium solution was used as a mordant to separate phases in well-polished samples.

The microhardness of the alloys was measured using a PMT-3 metallographic microscope. The density of the samples was determined by the pycnometric method; toluene was used as a working solution.

Electrical conductivity and thermo-EMF of $(In_2Se_3)_{1-x}(SrInSe_2)_x$ solid solutions were measured by the conventional direct current method in weak electric and magnetic fields (E < 10 V/cm, H < 10 kG) using a UA-1 electrometric amplifier UA-51-1 (Kolomiets, 1962; Glazov *et al*., 1969). The spectral dependence of the photoconductivity of $(In_2Se_3)_{1-x}(SrInSe_2)_x$ solid solutions was measured by the compensation method (Ryvkin, 1963).

## 3. Results and discussion

The alloys of the system were synthesized to study the possible chemical interaction in the $In_2Se_3$-$SrInSe_2$ system. The prepared alloys are moderately resistant to air and organic solvents. Strong acids ($HNO_3$, HCl) quickly decompose them.

Thermograms of the alloys were recorded in the temperature range of 1000-1200°C. As a result of the analysis, it was established that the thermograms of the samples contain two, three and four endothermic effects. The abundance of effects in the system corresponds to phase transitions of the $In_2Se_3$ compound.

To determine the microstructure of the samples, the microstructure of the alloys around the main components and in the intermediate part was studied. It has been established that in the $In_2Se_3$-$SrInSe_2$ system, a single-phase region was found (7-90 mol % $SrInSe_2$), whereas the remaining alloys were found to be two-phase ones. Figure 1 shows the microstructures of samples of the $In_2Se_3$-$SrInSe_2$ system with contents of 7, 20, 35 and 90 mol % $SrInSe_2$.

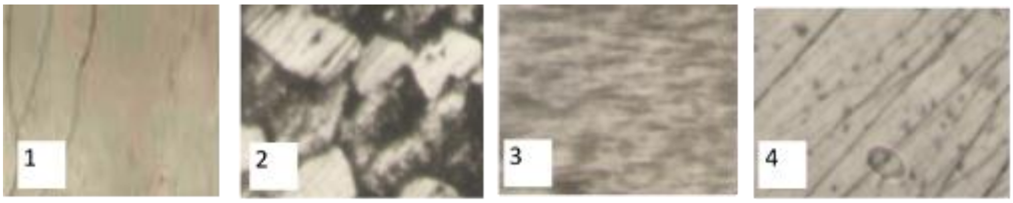


**Figure 1.** Microstructure of alloys in the $In_2Se_3$-$SrInSe_2$ system.
1-7, 2-20, 3-35, 4-90 mol % $SrInSe_2$

As can be seen from Figure 1, single-phase samples containing 7 and 90 mol % $SrInSe_2$ are solid solution alloys based on $In_2Se_3$ and $SrInSe_2$ compounds, respectively. A sample containing 30 mol % $SrInSe_2$ is a two-phase alloy. A sample containing 35 mol % $SrInSe_2$ is an eutectic alloy.

To confirm the results of differential thermal and microstructural analysis, X-ray diffraction patterns were taken of alloys containing 7, 70 and 90 mol % $SrInSe_2$ (Figure 2). It has been established that the existing diffraction lines in the diffraction patterns of single-phase alloys containing 7 and 90 mol % $SrInSe_2$ are identical to the diffraction lines of the compounds $In_2Se_3$ and $SrInSe_2$, respectively. These samples are solid solution alloys based on $In_2Se_3$ and $SrInSe_2$ compounds. As a result, it became clear that the diffraction lines of intermediate alloys consist of a mixture of diffraction lines of the original components. Its powder XRD result shows an alloy with 70 mol % $SrInSe_2$ is two-phase. That is, the $In_2Se_3$-$SrInSe_2$ system is quasi-binary. Thus, X-ray phase analysis confirms the results of DTA and MSA analyses.

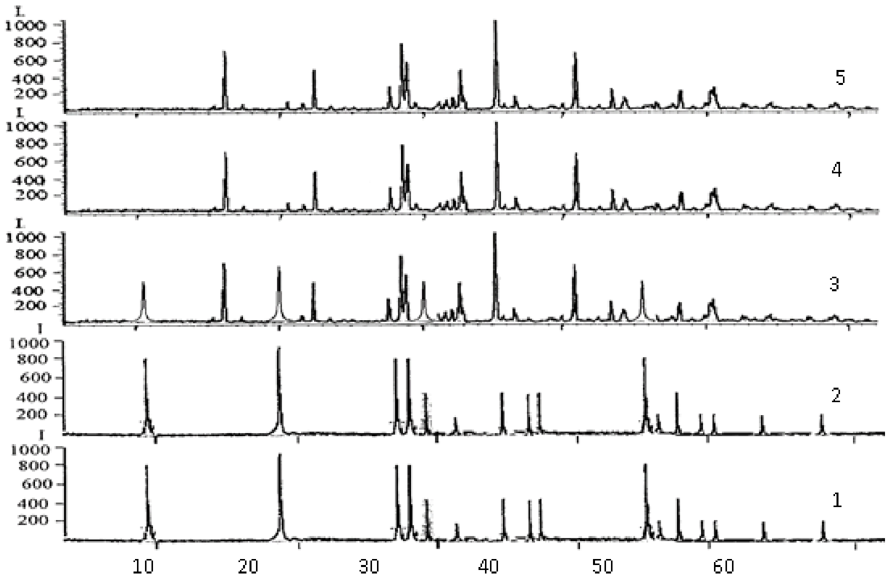


**Figure 2.** Diffraction patterns of alloys of the $In_2Se_3$-$SrInSe_2$ system
1- $In_2Se_3$, 2-7, 3-70, 4-90, 5-100 mol % $SrInSe_2$

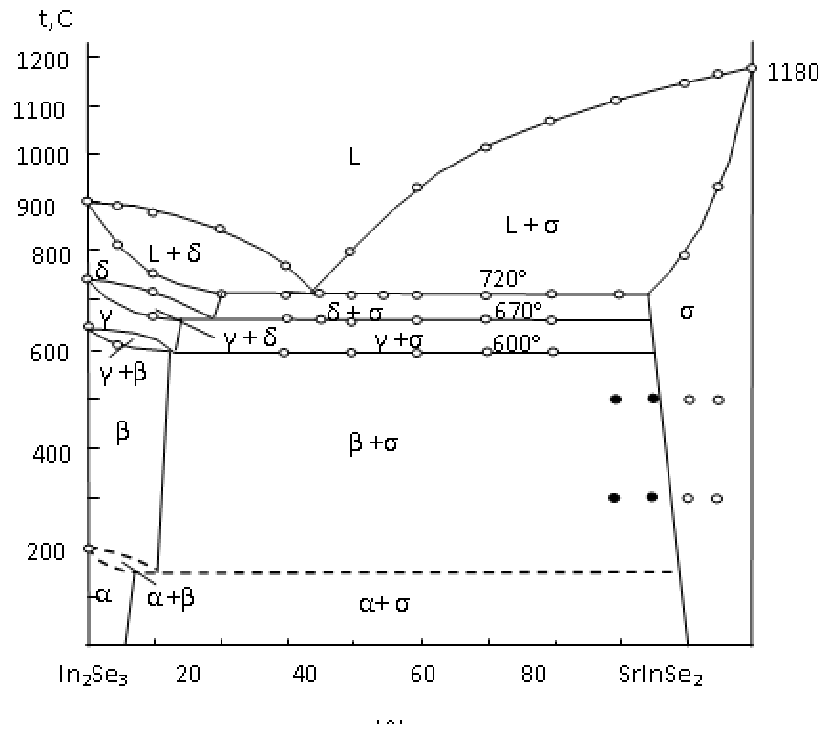


**Figure 3.** T-x phase diagram of the $In_2Se_3$-$SrInSe_2$ system

The T-x phase diagram of the $In_2Se_3$-$SrInSe_2$ system was constructed based on the results of physicochemical analysis methods (Figure 3).

As seen from Figure 3, the phase diagram of the system is of the eutectic type. Based on the starting components, there is a limited region of solid solutions. In a system based on $In_2Se_3$, solid solutions reach up to 7 mol % $SrInSe_2$. To determine the area of the solid solution based on the $SrInSe_2$ compound, alloys containing 3, 5, 10 and 15 mol % $In_2Se_3$ were synthesized, kept at 300 and 500°C for 150 hours and then directly cooled in ice water. Then their microstructural analysis was carried out. As a result, it became clear that the solubility based on $SrInSe_2$ extends up to 10 mol % $In_2Se_3$ at room temperature.

The microhardness measurements of alloys of the $In_2Se_3$-$SrInSe_2$ system show that two different microhardness values have been determined.

The dependence of some physicochemical properties of the alloys of the system on the composition is presented in Table 1. As can be seen from the table, the microhardness value (630-680) MPa corresponds to the microhardness of α-solid solutions based on $In_2Se_3$ and the value (1080-1130) MPa corresponds to the microhardness value σ-solid solutions based on the $SrInSe_2$ compound. The dependence of density on composition varies linearly.

The liquidus of the $In_2Se_3$-$SrInSe_2$ system consists of monovariant crystallization curves δ and σ of solid solutions. For the $In_2Se_3$ compound, there are phase transitions α↔β (200°C), β↔γ (650°C), γ↔δ (750°C). Alloys of the system in the range of 0-7 mol % $SrInSe_2$ and 90-100 mol % $SrInSe_2$ are single-phase. Two-phase alloys consisting of (α + σ) crystallize below the solidus line in the 7-90 mol % $SrInSe_2$ range. The eutectic formed in the system has a coordinate of 35 mol % $SrInSe_2$ and a temperature of 720°C.

**Table 1.** Compositions, DTA results, microhardness and density measurements of alloys of the $In_2Se_3$-$SrInSe_2$ system

| Composition, mol % | | Thermal effects,°C | Density, q/sm$^3$ | Microhardness, MPa | |
|---|---|---|---|---|---|
| | | | | α | σ |
| $In_2Se_3$ | $SrInSe_2$ | | | P=0,15 N | P=0,20 N |
| 100 | 0,0 | 900 | 5,67 | 630 | - |
| 95 | 5,0 | 610,820,900 | 5,69 | 650 | - |
| 90 | 10 | 670,730,750,890 | 5,60 | 670 | - |
| 80 | 20 | 720,850 | 5,55 | 670 | - |
| 70 | 30 | 600,660,720,775 | 5,51 | 680 | - |
| 65 | 35 | 670,720, | 5,40 | Eutec. | Eutec. |
| 60 | 40 | 600,670,720,800 | 5,45 | - | - |
| 50 | 50 | 600,670,720,930 | 5,39 | - | 1130 |
| 40 | 60 | 600,670,720,1020 | 5,35 | - | 1130 |
| 30 | 70 | 600,670,720,1070 | 5,29 | - | 1130 |
| 20 | 80 | 720,1100 | 5,23 | - | 1130 |
| 10 | 90 | 790,1140 | 5,19 | - | 1130 |
| 5,0 | 95 | 925,1160 | 5,16 | - | 1110 |
| 0,0 | 100 | 1180 | 5,13 | - | 1080 |

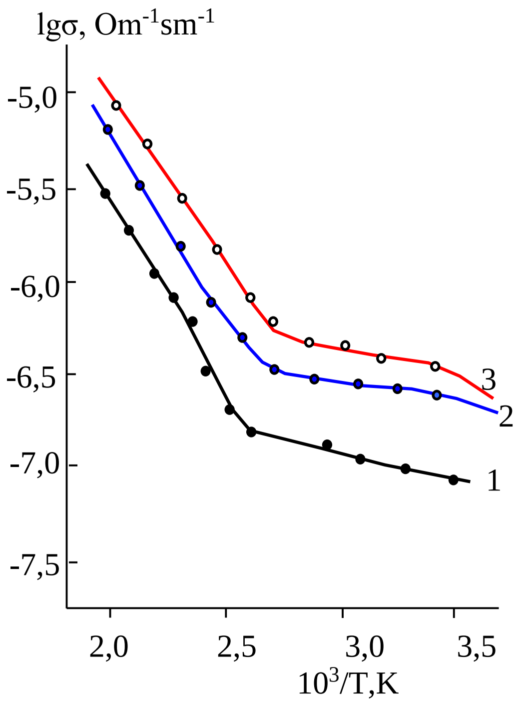


**Fig.4.** Temperature dependence of electrical conductivity (σ) $(In_2Se_3)_{1-x}(SrInSe_2)_x$(x = 0,01; 0,03; 0,05) solid solutions of alloys 1-1 mol %, 2-3 mol %, 3-5 mol % $SrInSe_2$

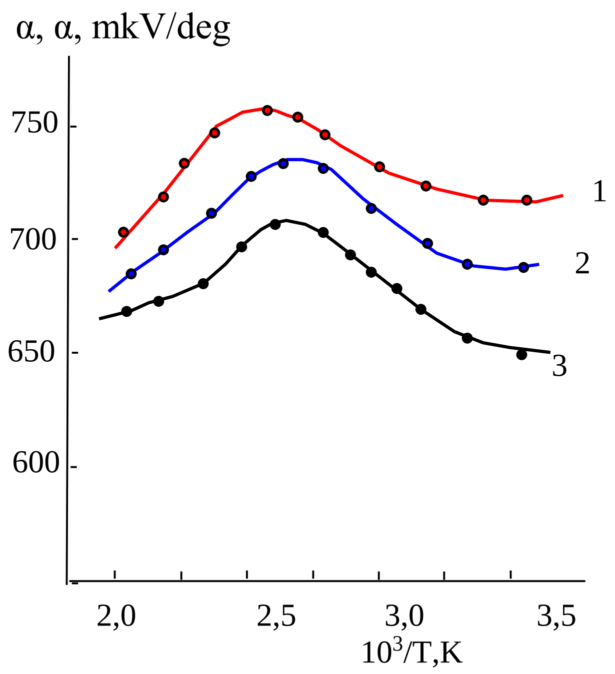


**Fig.5.** Temperature dependence of thermo-emf (α) $(In_2Se_3)_{1-x}(SrInSe_2)_x$ (x = 0,01; 0,03; 0,05) solid solutions of alloys 1-1 mol %, 2-3 mol %, 3-5 mol % $SrInSe_2$

When 1, 3, 5 mol % $SrInSe_2$ was added to the $In_2Se_3$ compound, its conductivity increased depending on the composition (Figure 4). When the $SrInSe_2$ compound was added to the $In_2Se_3$ compound, it penetrates between the layers of the $In_2Se_3$ compound. It participates in conductivity, which leads to an increase in electrical conductivity. Considering that the electrical conductivity value for n-type semiconductors was calculated using the following formula.

$$\sigma = \sigma_0 e^{\frac{E_g - E_n}{KT}},$$

where $E_n$ is the chemical potential. Then, the dependence σ~1/T will be entirely exponential at $\sigma_0$=const. With increasing temperature in the regions of the $(In_2Se_3)_{1-x}(SrInSe_2)_x$ solid solution, the electrical conductivity increases; these alloys are substances with semiconductor properties.

As a result of electrical conductivity measurements, it was established that the $(In_2Se_3)_{1-x}(SrInSe_2)_x$ solid solution alloys are n-type semiconductors. At room temperature, the electrical conductivity value of $SrInSe_2$ alloys containing 1, 3, 5 mol % is lgσ = -7.80 $Om^{-1}\cdot cm^{-1}$, lgσ =-6.85 $Om^{-1}\cdot cm^{-1}$ and lgσ =-6.40 $Om^{-1}\cdot cm^{-1}$ (Figure 4). In the 300-400 K temperature range, impurity conductivity is observed in all three alloys containing 1, 3 and 5 mol. % $SrInSe_2$. The intrinsic conductivity of the samples begins after 400 K-the value of the electrical conductivity of alloys containing 1, 3 and 5 mol. % $SrInSe_2$, at a temperature of 500 K lgσ= -5.50 $Om^{-1}.cm^{-1}$, lgσ=-5.75 $Om^{-1}.cm^{-1}$ and lgσ= -5.90 $Om^{-1}$ $cm^{-1}$.

Figure 5 shows the temperature dependence of thermo-EMF of solid solutions $(In_2Se_3)_{1-x}(SrInSe_2)_x$ (x=0.01; 0.03; 0.05). As can be seen from Figure 5, the maximum significance of thermo-EMF reaches the value α=715 μV (5 mol %), α= 735 μV (3 mol %), α=770 μV (1 mol %), after which it begins to decrease sharply.

The sample of $(In_2Se_3)_{1-x}(SrInSe_2)_x$ (x=0.01;0.03;0.05) solid solutions to measure the photoconductivity have to be selected as small as possible because the $\vartheta$ sensitivity of the samples is inversely proportional to the d thickness.

$$\vartheta = \frac{A}{d(1-\exp(-kd))}.$$

Their homogeneity is essential when selecting contacts since photoconductivity parameters (lifetime, quantum energy, etc.) can change due to the impact on the zones. Therefore, the length of the samples between the electrodes should be increased so that the influence of the contacts is kept to a minimum.

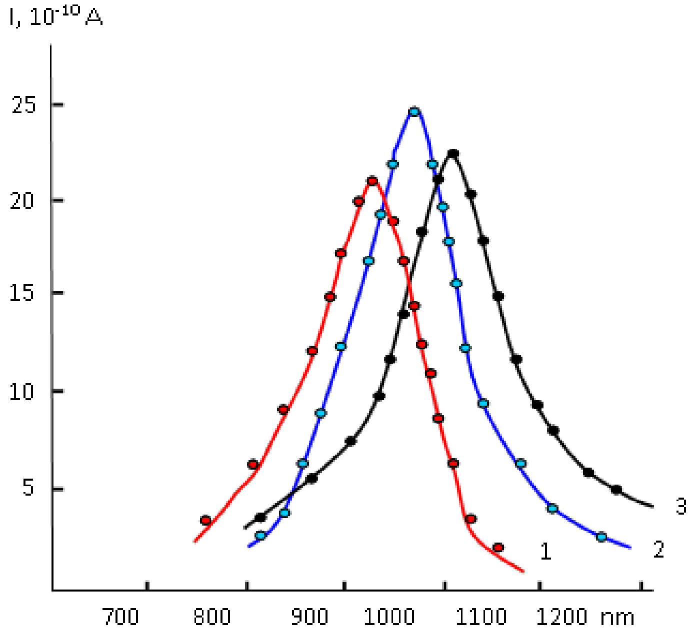


**Figure 6.** Spectral dependence of the photoelectric current of solid solution samples $(In_2Se_3)_{1-x}(SrInSe_2)_x$ (x=0.01;0.03;0.05). (1-1 mol %; 2-mol %; 3-5 mol % $SrInSe_2$)

Measurements of the photoelectric properties of $(In_2Se_3)_{1-x}(SrInSe_2)_x$ (x=0.01;0.03;0.05) showed that adding 1 mol % and 3 mol % $SrInSe_2$ to the $In_2Se_3$ compound increases the magnitude of the photocurrent (Figure 6). The maximum photocurrent was observed in a sample with a concentration of 3 mol % $SrInSe_2$. When added to the composition, 5 mol % $SrInSe_2$ photoconductivity decreases (Figure 6). The compensation of electrical charges can explain it. These samples were found to be sensitive to 800-1200 nm wavelengths. The bandgap based on maximum photoconductivity can be calculated using the following formula:

$$\Delta E = hs/\lambda = 1.24/\lambda.$$

Maximum photoconductivity was observed at a wavelength of 950 nm. As can be seen from Figure 5, when adding 1, 3 and 5 mol % $SrInSe_2$ to the $In_2Se_3$ compound, the maximum value of the photoelectric conductivity of the sample shifted slightly to the longer wavelength side.

## 4. Conclusion

The chemical interaction in the $In_2Se_3$-$SrInSe_2$ system was studied using the following methods: differential thermal analysis (DTA), X-ray diffraction (XRD), microstructural analysis (MSA), as well as density and microhardness measurements and a T-x phase diagram was constructed. The phase diagram of the system is quasi-binary, of the eutectic type, characterized by the formation of a solid solution region based on the initial components. The combined crystallization of the compounds $In_2Se_3$ and $SrInSe_2$ ends at the double eutectic point; the eutectic composition is 35 mol % $SrInSe_2$, with a melting point of 720°C. At room temperature, solid solutions based on the $In_2Se_3$ compound reach up to 7 mol % $SrInSe_2$ and those based on $SrInSe_2$ up to 10 mol % $In_2Se_3$. The dependence of the density and microhardness of alloys of the $In_2Se_3$-$SrInSe_2$ system on composition has been studied. Electrical conductivity, thermo-Emf and photoelectric properties of solid solutions $(In_2Se_3)_{1-x}(SrInSe_2)_x$ (x=0.01; 0.03; 0.05) were studied.

## References

Aliyev, I.I., Aliyev, O.M. & Mahammadrahimova, R.S. (2019). Phaseformation in the system $InAs_2S_3Se$-$InAs_2Se_3S$ and properties of obtained phases. *Azerbaijan Chemical Journal*, 2, 44-47. https://doi.org/10.32737/0005-2531-2019-2-44-47

Aliyev, I.I., Mamedova, N.A., Sadigov, F.M., Sadigov, N.M. & Melikova, I.G. (2020). Study of chemical interaction in the $Sb_2Te_3$-InSe system and properties of the resulting phases. *Journal of Inorganic Chemistry*, *65*(10), 1386-1391. (In Russian).

Andreev, O.B., Kertman, A.B. & Bamburov, V.G. (1991). Phase equilibria in the $La_2S_3$-SrS and $Nd_2S_3$-SrS systems. *Journal of Inorganic Chemistry*, *36(*1), 253-257. (In Russian).

Andreev, O.V., Mitroshin, O.Y., Khritokhin, N.A. & Razumkova, I.A. (2008). Phase equilibria laws in the SrS-$Lu_2S_3$ systems. *Russian Journal of Inorganic Chemistry*, 53, 440-445.

Askerov, S.G., Abdullayeva, L.K., & Hasanov, M.G. (2020). Study of electrophysical properties of metal–semiconductor contact by the theory of complex systems. *Journal of Semiconductors*, *41*(10), 102101.

Chartier, C., Barthou, C., Benalloul, P., Chenot, S. & Frigerio, J.M. (2003). Structural and luminescent properties of green emitting $SrGa_2S_4$:Eu thin films prepared by RF-sputtering. *Journal of Crystal Growth*, *256*(3-4), 305-316.

Glazov, V.M., Okhotin, A., Pushkarskiy, N., Borovikova, R. & Smirnov, R. (1969). *Methods of Investigation of Thermoelectric Properties of Semiconductors*. Moscow: Atomnzdat, 176. (In Russian).

Ho, C.H., Lin, C.H., Wang, Y.P., Chen, Y.C., Chen, S.H. & Huang, Y.S. (2013). Surface oxide effect on optical sensing and photoelectric conversion of α-In2Se3 hexagonal microplates. *ACS Applied Materials & Interfaces*, *5*(6), 2269-2277. https://doi.org/10.1021/am400128e

Island, J.O., Blanter, S.I., Buscema, M., van der Zant, H.S. & Castellanos-Gomez, A. (2015). Gate controlled photocurrent generation mechanisms in high-gain $In_2Se_3$ phototransistors. *Nano Letters*, *15*(12), 7853-7858. https://doi.org/10.1021/acs.nanolett.5b02523

Jacobs-Gedrim, R.B., Shanmugam, M., Jain, N., Durcan, C.A., Murphy, M.T., Murray, T.M. & Yu, B. (2014). Extraordinary photoresponse in two-dimensional $In_2Se_3$ nanosheets. *ACS Nano*, *8*(1), 514-521. https://doi.org/10.1021/nn405037s

Kolomiets, N.B. (1962). Measurement of thermoelectromotive force and resistivity in the temperature range from 20 to 1900°C. *Factory Laboratory*, *28*(2), 238-240.

Liu, K., Zhang, T., Dang, B., Bao, L., Xu, L., Cheng, C. & Yang, Y. (2022). An optoelectronic synapse based on α-$In_2Se_3$ with controllable temporal dynamics for multimode and multiscale reservoir computing. *Nature Electronics*, *5*(11), 761-773. https://doi.org/10.1038/s41928-022-00847-2

Lyakishev, N.P. (2001). *State Diagrams of Binary Metal Systems*. Handbook, 872.

Mahammadrahimova, R.S., Aliyev, I.I., Aliyev, O.M. & Babanly, K.N. (2018). Phase equilibrium in quasi-ternary system $InAs_2SSe_3$-$InAs_2S_3Se$-$In_3As_2S_3Se_3$. *Azerbaijan Chemical Journal*, 4, 49-54.

Mammadov, F.M. (2019). Phase diagram of the FeSe-$In_2Se_3$ system. *Azerbaijan Chemical Journal*, 3, 62-67. https://doi.org/10.32737/0005-2531-2019-3-62-67

Ryvkin, S.M. (1963). *Photoelectric Phenomena In Semiconductors*. Moscow, Fizmatgiz, 494. (In Russian).

Tagiev, B.G., Tagiev, O.B., Dzhabbarov, R.B., Musaeva, N.N. & Gasimov, U.F. (2000). Photoluminescence in $Ca_4Ga_2S_7$:$Ce^{3+}$ and $Ca_4Ga_2S_7$:$Pr^{3+}$ compounds. *Inorganic Materials, 36*(1), 3-6. (In Russian).

Van Haecke, J.E., Smet, P.F. & Poelman, D. (2004). The influence of source powder composition on the electroluminescence of $Ca_{1-x}Sr_xS$:Eu thin films. *Spectrochimica Acta Part B: Atomic Spectroscopy*, *59*(10-11), 1759-1764.

Van Haecke, J.E., Smet, P.F. & Poelman, D. (2005). The formation of $Eu^{2+}$ clusters in saturated red $Ca_{0.5}Sr_{0.5}S$:Eu electroluminescent devices. *Journal of the Electrochemical Society*, *152*(12), H225.

Wauters, D., Poelman, D., Van Meirhaeghe, R.L. & Cardon, F. (2000). Photoluminescent, electroluminescent and structural properties of CaS: Cu and CaS: Cu, Ag thin films. *Journal of Physics: Condensed Matter*, *12*(16), 3901.

Wu, J., Newman, D. & Viney, I.V. (2002). Study on relationship of luminescence in CaS:Eu, Sm and dopants concentration. *Journal of Luminescence*, *99*(3), 237-245.

Xue, F., He, X., Liu, W., Periyanagounder, D., Zhang, C., Chen, M. & Zhang, X. (2020). Optoelectronic ferroelectric domain-wall memories made from a single Van Der Waals ferroelectric. *Advanced Functional Materials*, *30*(52), 2004206. https://doi.org/10.1002/adfm.202004206

Yagubov, N.I, Sultanova, A.N., Farzaliyeva, Z.A. & Aliyeva, K.I. (2022). Chemical interaction in the $Sr_3In$-SrSe System. *Annali d'Italia*, 37, 6-8. https://doi.org/10.5281/zenodo.7357636

Yagubov, N.I., Sultanova, A.N. & Aliyev, I.I. (2023b). Studying chemical interaction in the Ga-SrSe system. *Proceedings Chemistry*, 2, 78-82. https://doi.org/10.61413/Pfhg7389

Yagubov, N.I., Sultanova, A.N., Aliyev, I.I., Gurbanov, G.B., Suleymanova, M.N., Alizadeh, F.A. & Bayramova, A.G. (2024). Synthesis of alloys of the $In_2Se_3$-$SrInSe_2$ system and investigation of the region of solid solutions. *Dedicated to the 101st Anniversary of the Birth of National Leader Heydar Aliyev International Scientific Conference of Current Problems of Modern Natural and Economic Sciences*, 27-29. Ganja. (In Azerbaijan).

Yagubov, N.I., Sultanova, A.N., Aliyev, I.I. & Ahmedova, C.A. (2023a). Nature of chemical interaction in the $SrGaSe_2$-SrSe. *News of Baku University, Series of Natural Sciences*, 4, 12-19. (In Azerbaijan).

Zhai, T., Fang, X., Liao, M., Xu, X., Li, L., Liu, B. & Golberg, D. (2010). Fabrication of high-quality $In_2Se_3$ nanowire arrays toward high-performance visible-light photodetectors. *ACS Nano*, *4*(3), 1596-1602. https://doi.org/10.1021/nn9012466

Zhou, F., Zhou, Z., Chen, J., Choy, T.H., Wang, J., Zhang, N. & Chai, Y. (2019). Optoelectronic resistive random access memory for neuromorphic vision sensors. *Nature Nanotechnology*, *14*(8), 776-782. https://doi.org/10.1038/s41565-019-0501-3